Electronic Supplementary Material (ESI) for Physical Chemistry Chemical Physics.

Supporting Information file

Effect of solvent vapor annealing on optical properties and surface adhesion of conjugated D:A thin films

Tainã Reges Casagrande[1], Juscelino Valter Barbosas Júnior[1], Jaqueline Cristine Desordi[1], Mariana Richelle Pereira da Cunha[2], Anderson Emanuel Ximim Gavim[2], Luciano Nassif Vidal[3], Paula Cristina Rodrigues[3], Indrani Coondoo[4], Douglas J. Coutinho[2], Roberto Mendonça Faria[1-3], Andreia Gerniski Macedo[1]

[1]*Graduate Program in Physics and Astronomy, Federal University of Technology, Curitiba – PR – Brazil*

[2]*Institute of Physics, University of São Paulo, São Carlos – SP – Brazil*

[3] *Graduate Program in Chemistry, Federal University of Technology, Curitiba – PR – Brazil*

[4]*Department of Physics, University of Aveiro, Aveiro - Portugal*

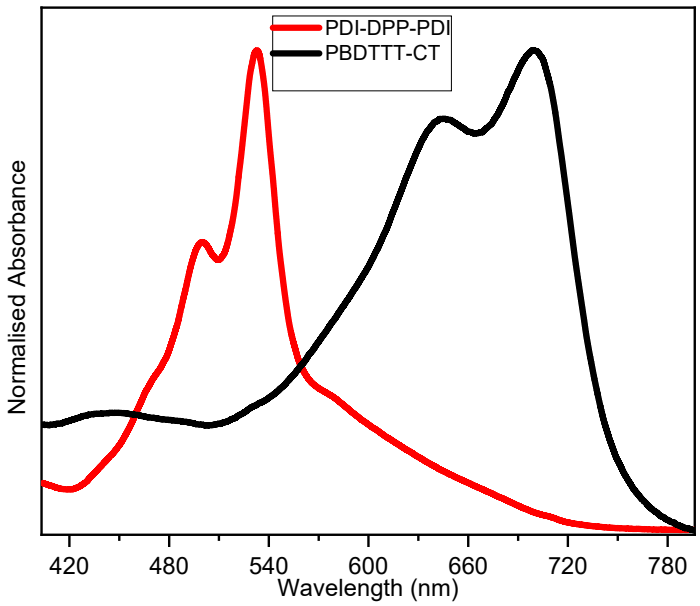

Figure S1 - Normalised absorbance spectra acquired from PDI-DPP-PDI and PBDTTT-CT solutions in CB.

Density Functional Theory Results

This section presents DFT and TD-DFT results of structure and electronic absorption spectrum for PDI-DPP-PDI, some oligomers of PBDTTT-CT, and the aggregated PDI-DPP-PDI:2BDTTT-CT, which involves a dimer of PBDTTT-CT. As detailed in the *Computational Details* section of the main document, all geometry optimizations were performed at the ωB97X-D3/def2-SVP level, including the C-PCM solvation with chloroform as solvent. The ground state equilibrium geometries of PDI-DPP-PDI, 4BDTTT-CT (i.e., the tetramer), and PDI-DPP-PDI:2BDTTT-CT are shown in **Figures S2** and **S3**. Note that methyl groups substituted the alkyl side chains to save computational resources.

To select a proper level of theory capable of delivering a good agreement between the TD-DFT and observed absorption spectrum, that property was computed at the ωB97X-D3/def2-SVP/C-PCM equilibrium geometries using different basis sets and exchange-correlation (XC) functionals. To assess the influence of the basis sets size on the absorption spectra of PDI-DPP-PDI and 3BDTTT-CT (trimer), those spectra were calculated using the ma-def2-SVP and ma-def2-TZVP sets, combined with the ωB97X-D3 and M06-2X Minnesota functional (REF). Because the absorption spectra of the solutions were recorded using chlorobenzene as the solvent, the TD-DFT properties were computed using the SMD solvation model with chlorobenzene. The absolute transition intensities, given as oscillator strengths, were further normalized by setting the most intense transition to unit intensity. According to **Figure S4**, the spectra of both the molecule and trimer are slightly shifted toward the low-energy domain when calculated with the larger basis set, with negligible differences observed in the absorption bands' relative intensities. On the other hand, the number of basis functions nearly doubles from ma-def2-SVP to ma-def2-TZVP. Thus, we decided on the cost-effective ma-def2-SVP basis to compute the vertical excitation energies and oscillator strengths of 4BDTTT-CT and PDI-DPP-PDI:2BDTTT-CT systems, which demand higher computer resources. In **Figure S5**, it is shown the absorption spectra of PDI-DPP-PDI and 3BDTTT-CT in chlorobenzene obtained using the ωB97X-D3, M06, and M06-2X functionals, combined with the ma-def2-SVP basis set. It can be seen that the relative intensity between the two dominant bands in the molecule and trimer spectra is little affected by the XC-functional used. However, the excitation energies are very sensitive to that choice. According to **Figure S1**, the two leading bands of the polymer are observed around 670 nm, and for the molecule, they are situated around 510 nm. Clearly, the M06 spectra are closer to the experimental results, and the absorption spectra considered in the main document were obtained using this functional.

To estimate the absorption spectrum of PBDTTT-CT, we have computed the spectra of some oligomers observing their convergence with respect to the number of monomer units. These results are given in **Figure S6** and were obtained with two different XC functionals (M06-2X and ωB97X-D3) combined with the ma-def2-SVP basis and the SMD solvation with CB as the

solvent. Despite the difference between the spectra of 3BDTTT-CT and 4BDTTT-CT, these are far less pronounced than those observed when comparing the spectra of the dimer and trimer. Thus, we consider that 4BDTTT-CT has enough units to be a suitable representation of the absorption spectrum of PBDTTT-CT.

Aiming to explain the nature of the absorption band centered at 580 nm, originating after de SVA treatment, we decided to calculate the electronic spectra of the PDI-DPP-DPI:2BDTTT-CT aggregated, whose optimized structure is shown in **Figure S3**. More excited states need to be calculated for that system to cover the energy window corresponding to the visible range adequately. However, the amount of RAM required to perform such a calculation was beyond the resources available to our research group. To circumvent this limitation, we performed those calculations using the Gaussian 16 suite of programs. Therefore, the TD-DFT properties of PDI-DPP-PDI, 4PBDTTT-CT, and PDI-DPP-DPI:2BDTTT-CT were (re)calculated at the M06/6-31++G(d,p) level with the SMD solvation model. According to **Figure S7**, the differences between the UV-vis spectra evaluated using orca (M06/ma-def2-SVP/SMD level) and Gaussian 16 are negligible. To simplify the analysis of the electronic spectra, we found it helpful to plot the contribution of each transition to the resulting bands (**Figure S8**) to select the most relevant states to include detailed information concerning intensities and orbitals involved. The corresponding oscillator strengths and a qualitative attribution based on Natural Transition Orbitals are available in **Table S1**. In addition, the most significant NTOs related to the 572 nm band of PDI-DPP-PDI:2BDTTT-CT are shown in **Figures S9** and **S10**.

An additional concern on the PDI-DPP-PDI:2BDTTT-CT complex is the Basis Set Superposition Error (BSSE), i.e., proximity between these molecules may result in non-physical changes in the electronic energy levels of each one due to incompleteness of the atomic basis sets. To assess whether the basis set of PDI-DPP-PDI significantly overlaps the 2BDTTT-CT fragment and vice-versa, we computed the absorption of spectra of each molecule with and without including those basis sets relating to the other piece. In other words, when simulating the spectrum of PDI-DPP-PDI with the corresponding ghost atoms of 2BDTTT-CT, those electrons and the nuclei relating to the 2BDTTT-CT portion were deleted, remaining only the basis functions centered at the nuclei positions. According to **Figure S11**, the difference between the spectra with/without ghost atoms is negligible; thus, we conclude that the absorption spectrum of PDI-DPP-PDI:2BDTTT-CT does not suffer from BSSE.

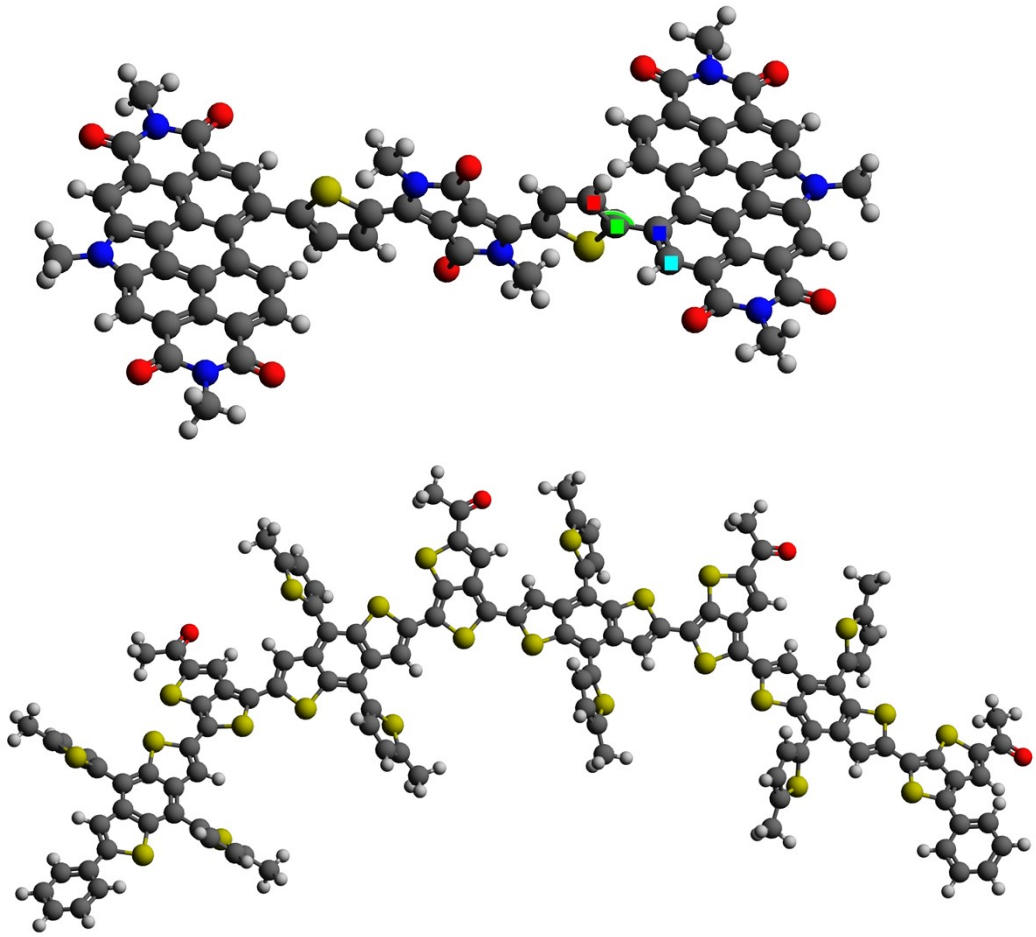

Figure S2 - Optimized geometries of PDI-DPP-PDI (top) and 4BDTTT-CT (bottom) with the alkyl side chains replaced with methyl groups.

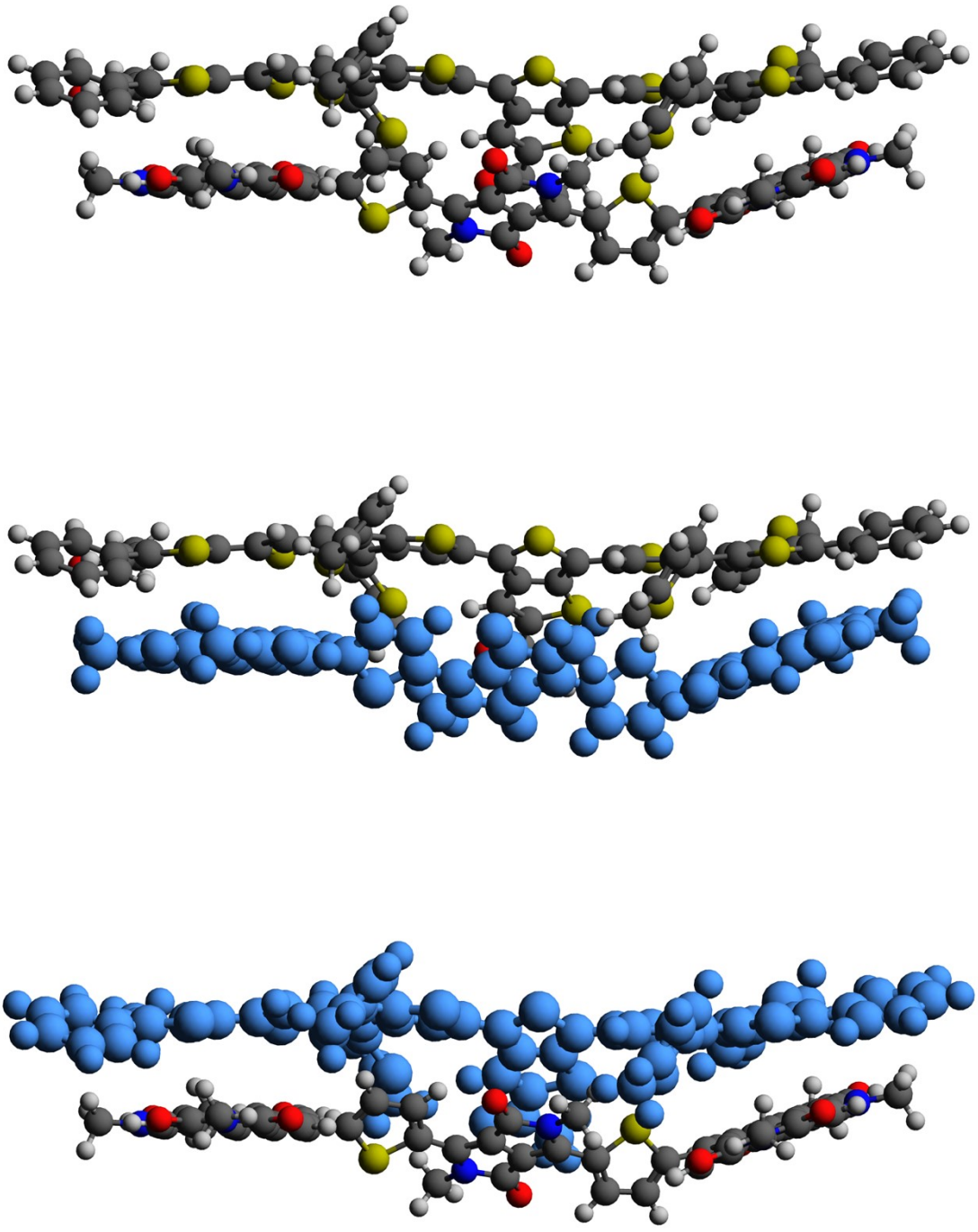

Figure S3 - Optimized geometry of PDI-DPP-PDI:2BDTTT-CT aggregated (top). In the middle, all atoms and bonds of the PDI-DPP-PDI portion are highlighted in blue. The same is done for 2BDTTT-CT at the bottom.

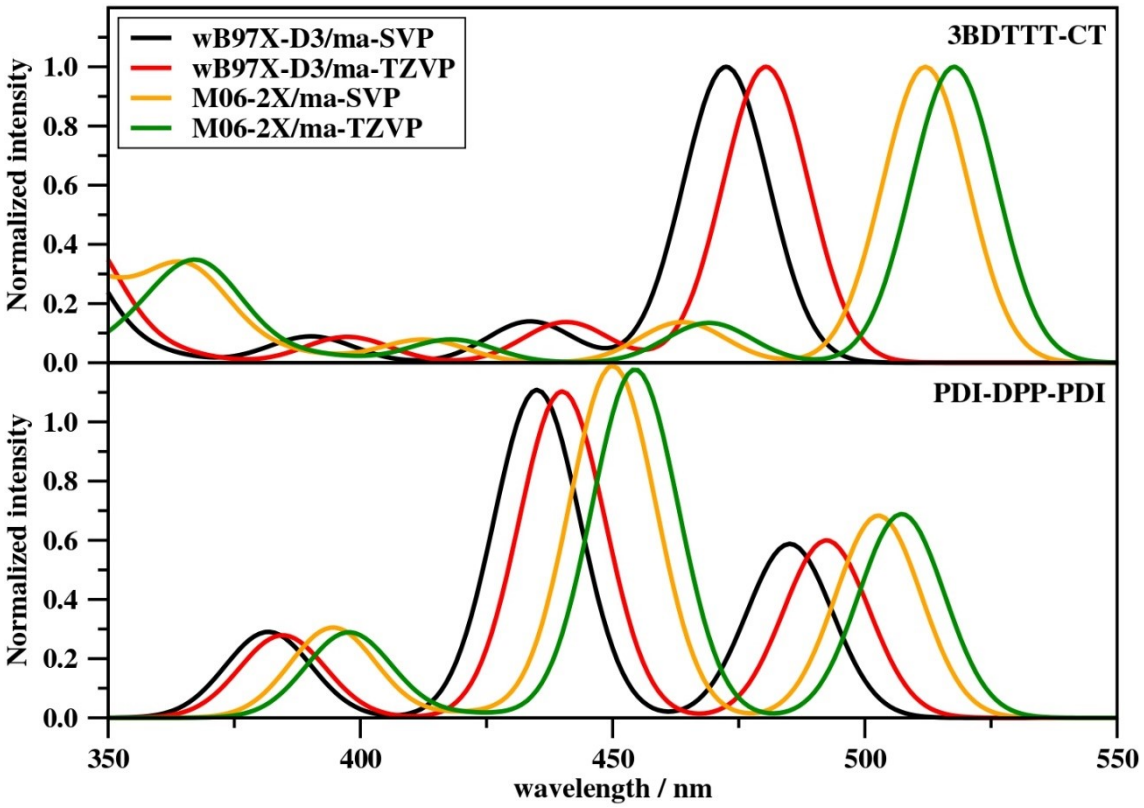

Figure S4 - Effect of different basis sets on the PDI-DPP-PDI and PBDTTT-CT (its trimer) absorption spectra in CB obtained using two different XC-functionals.

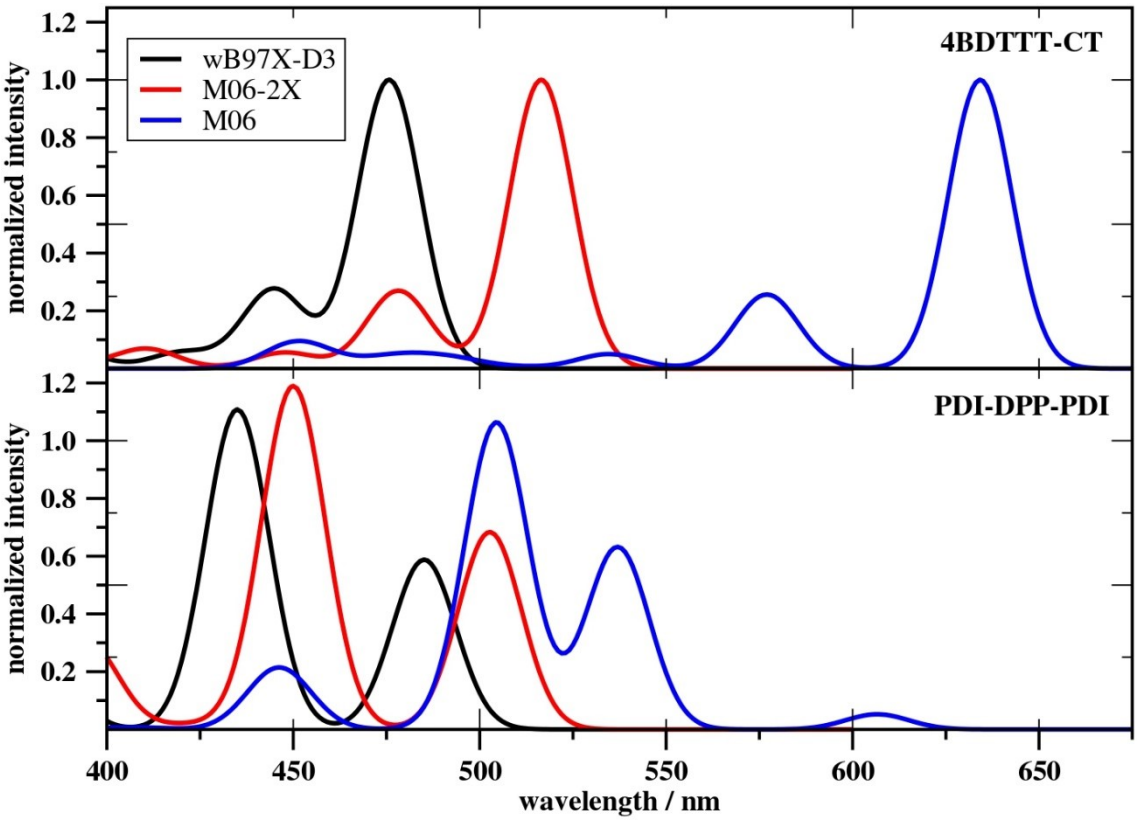

Figure S5 - Dependence of the XC-functional on the PDI-DPP-PDI and 4BDTTT-CT (tetramer) absorption spectra in CB. The basis set used was the ma-def2-SVP.

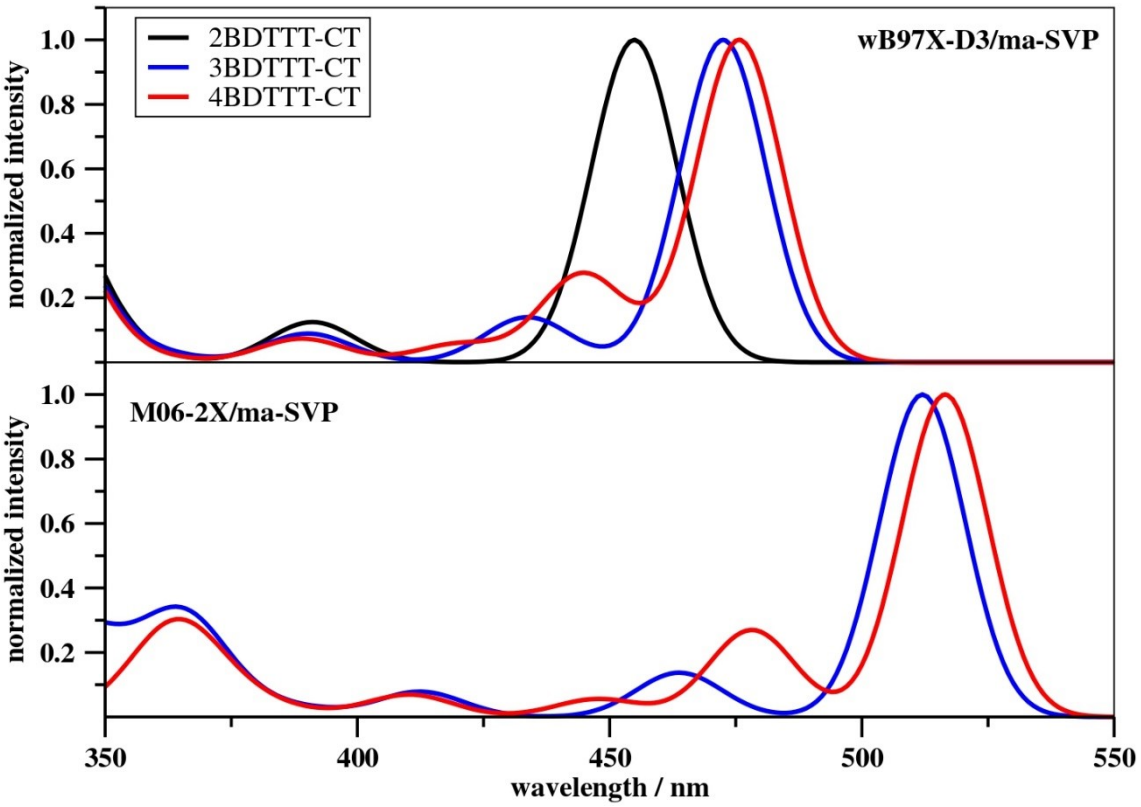

Figure S6 - Absorption spectra of some oligomers of PBDTTT-CT in CB computed using two different XC-functionals.

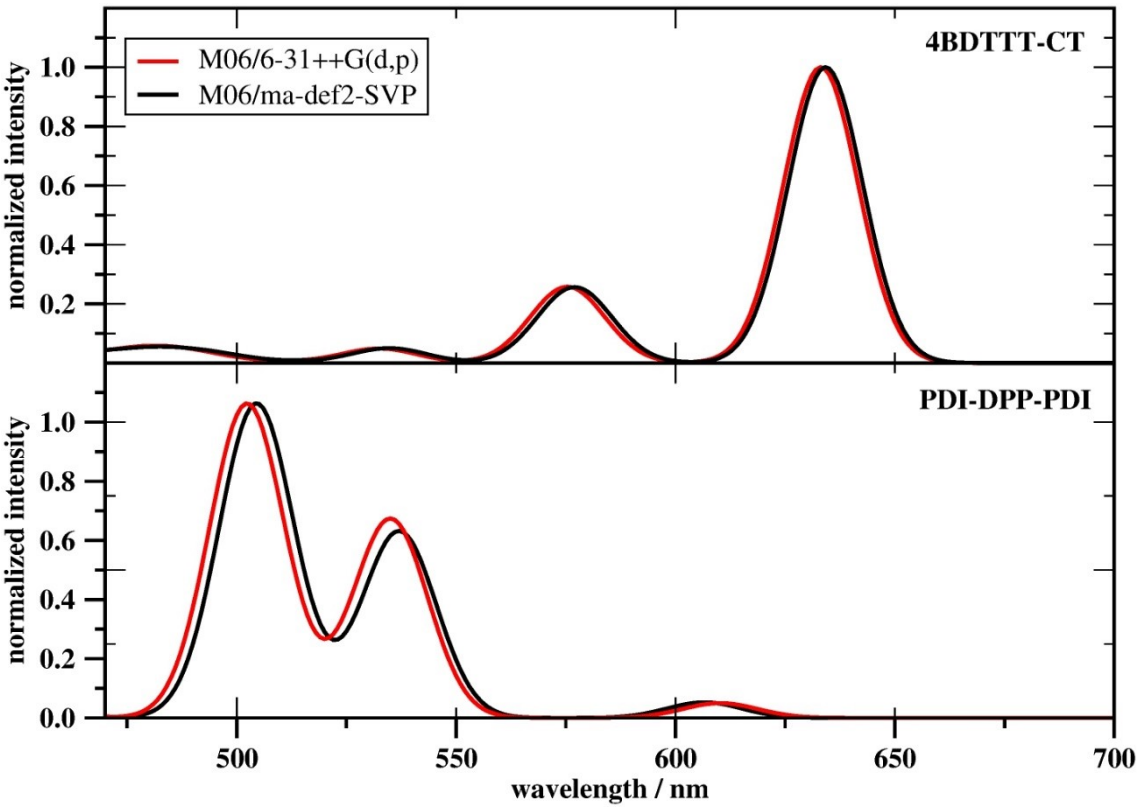

Figure S7 – Comparison of the absorption spectra of PDI-DPP-PDI and 4BDTTT-CT obtained with two different basis sets.

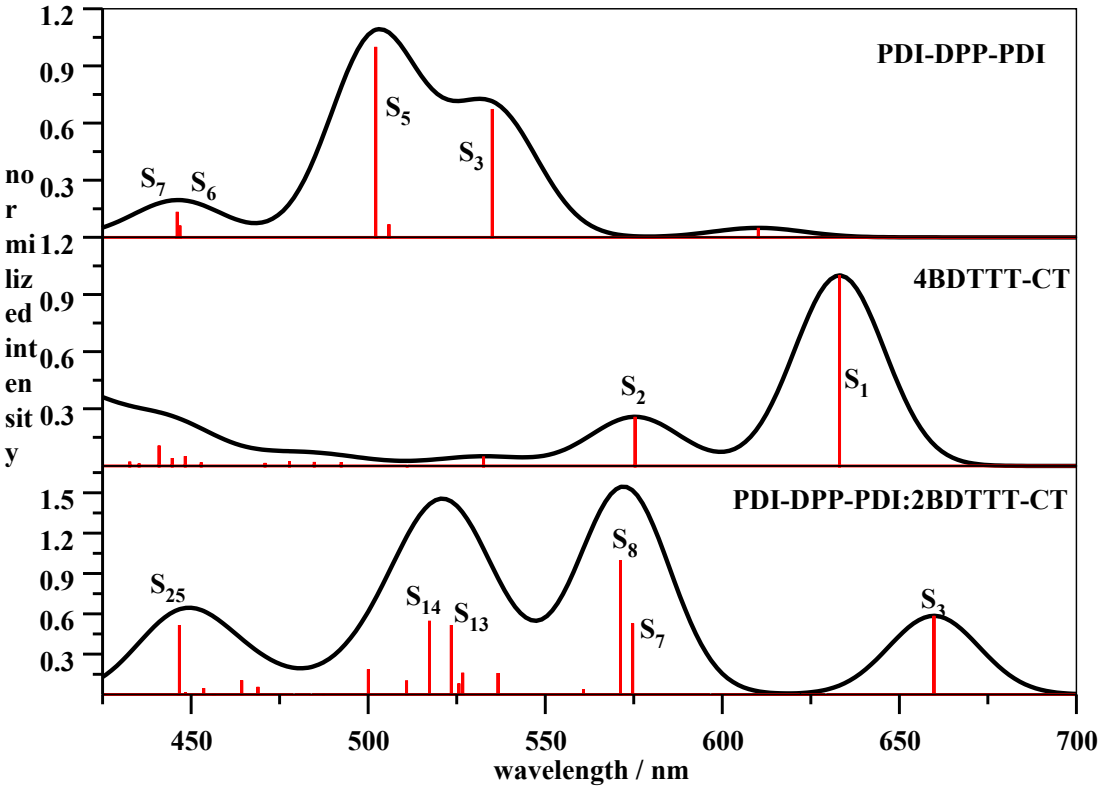

Figure S8 - Main electronic transitions contributing to the absorption spectra of PDI-DPP-PDI, 4BDTTT-CT, and PDI-DPP-PDI:2BDTTT-CT computed at the M06/6-31++G(d,p)/SMD level of theory.

Table S1 - TD-DFT vertical excitation wavelength (nm) and oscillator strength of singlet electronic transitions.[a]

State	Wavelength	Osc. Strength	NTO(attrib.)[b]		NTO(attrib.)	Weight
PDI-DPP-PDI						
S_3	535.03	1.0100	T-DPP-T	→	T-DPP-T	0.9302
S_5	502.11	1.4988	PDI_a	→	PDI_a	0.6868
			PDI_b	→	PDI_b	0.2483
S_6	446.82	0.0926	PDI_a	→	PDI_a	0.9285
S_7	446.08	0.2010	PDI_b	→	PDI_b	0.9263
4BDTTT-CT						
S_1	633.12	3.1751	BDT-TT	→	BDT-TT	0.8557
S_2	575.38	0.8185	BDT-TT	→	BDT-TT	0.5015
			BDT-TT	→	BDT-TT	0.4696
PDI-DPP-PDI:2BDTTT-CT						
S_3	659.76	0.5383	T-DPP-T	→	PDI-T-DPP-T-PDI	0.9552
S_7	574.69	0.4866	BDT-TT	→	PDI-T	0.6466
			BDT-TT	→	BDT-TT	0.3175
S_8	571.24	0.9201	BDT-TT	→	BDT-TT	0.6178
			BDT-TT+DPP	→	PDI	0.3443
S_{13}	523.49	0.4754	T-DPP-T	→	T-DPP-T-PDI	0.6595
			PDI	→	T-DPP-T-PDI	0.6595
S_{14}	517.31	0.5045	PDI	→	PDI	0.7191
			T-DPP-T	→	T-DPP-T	0.2223
S_{25}	446.70	0.4752	BDT-TT	→	BDT-TT	0.7335
			PDI_a	→	PDI_b	0.1494

[a] M06/6-31++G(d,p)/SMD level of theory. The solvent is chlorobenzene for PDI-DPP-PDI and PBDTTT-CT and chloroform for the aggregated.

[b] T = Thiophene; PDI_a = one of the PDI units; PDI_b = the other PDI unit; BDT = benzothiophene; TT = thienothiophene.

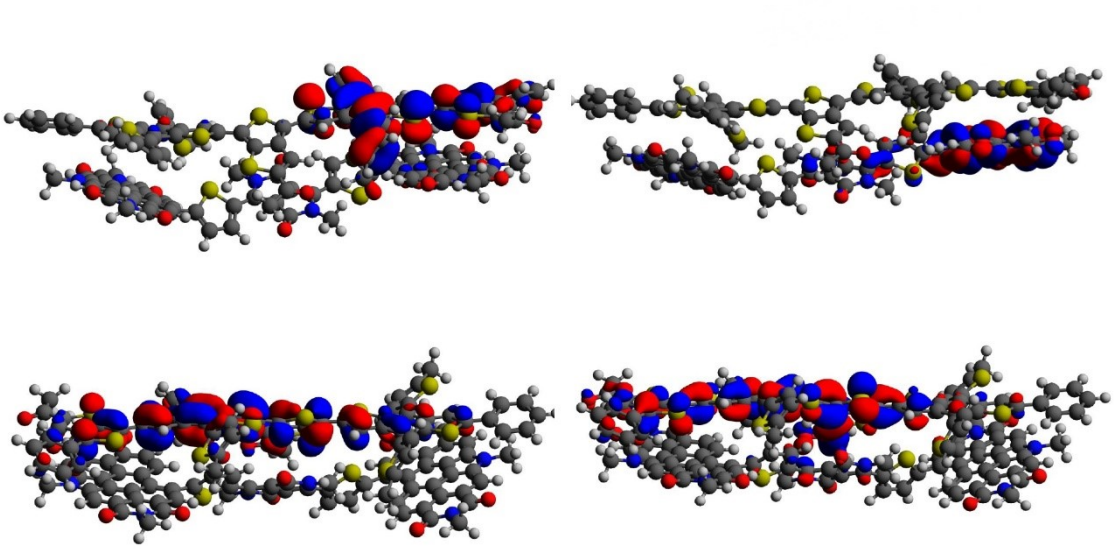

Figure S9 - Main NTOs involved in the singlet electronic transition $\mathbf{S_0 \rightarrow S_7}$ of the PDI-DPP-PDI:2BDTTT-CT aggregated. Starting orbitals are shown on the left side, and the corresponding ending orbitals are placed on the right. The PDI-DPP-PDI molecule is located below 2BDTTT-CT.

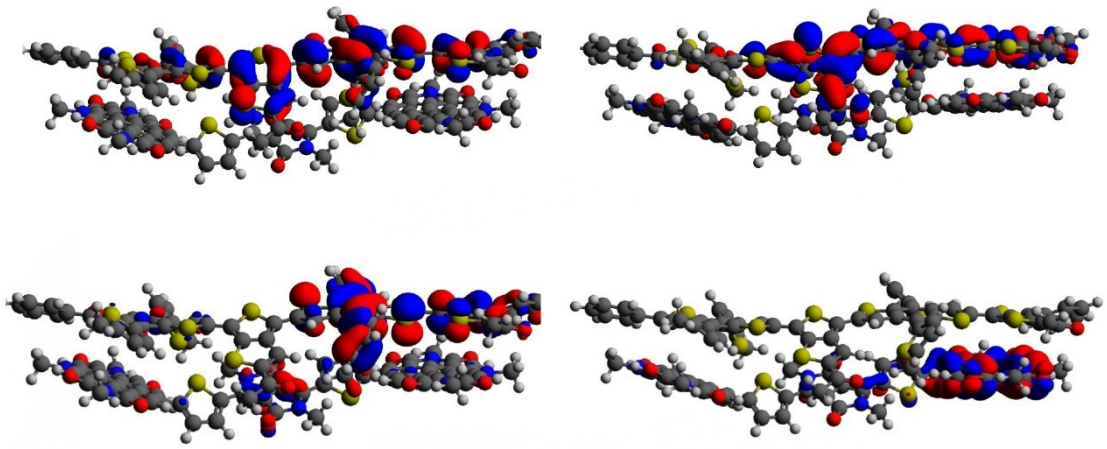

Figure S10 - Main NTOs involved in the singlet electronic transition $\mathbf{S_0 \rightarrow S_8}$ of the PDI-DPP-PDI:2BDTTT-CT aggregated. Starting orbitals are shown on the left side, and the corresponding ending orbitals are placed on the right. The PDI-DPP-PDI molecule is located below 2BDTTT-CT.

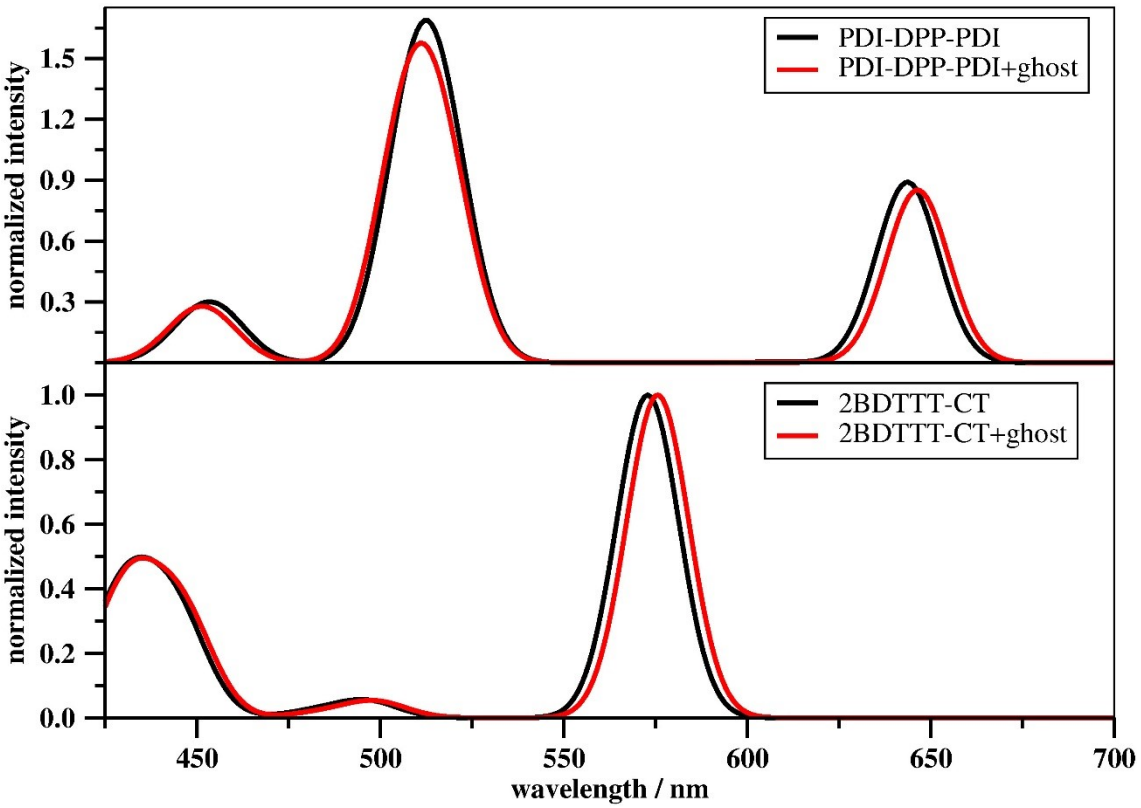

Figure S11 – M06/6-31++G(d,p)/SMD absorption spectra of PDI-DPP-PDI and 2BDTTT-CT calculated with (+ghost) and without ghost atoms to assess the extension of BSSE error.

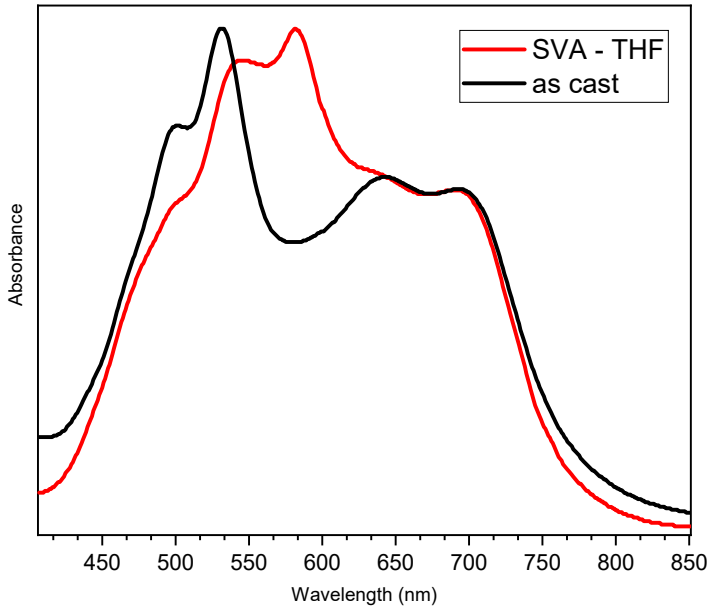

Figure S12 - Normalised absorbance spectra acquired from PBDTTT-CT:PDI-DPP-PDI films, being as cast (red line) and after SVA during 10 minutes in the vapour of THF solvent (black line).

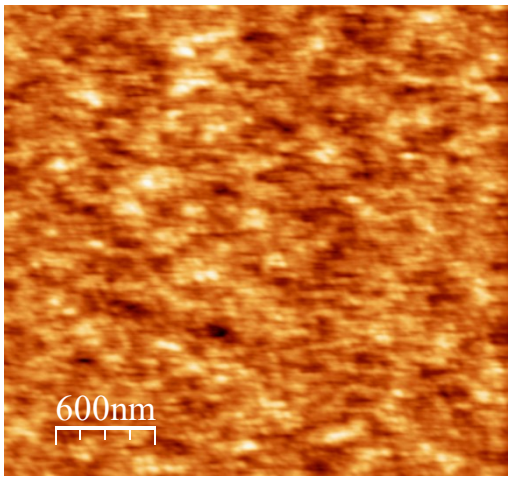

Figure S13 – AFM image acquired from SVA treated PBTTTT-CT:PDI-DPP-PDI with the vapor of THF, the calculated value of Rq is equal to 1.3 nm

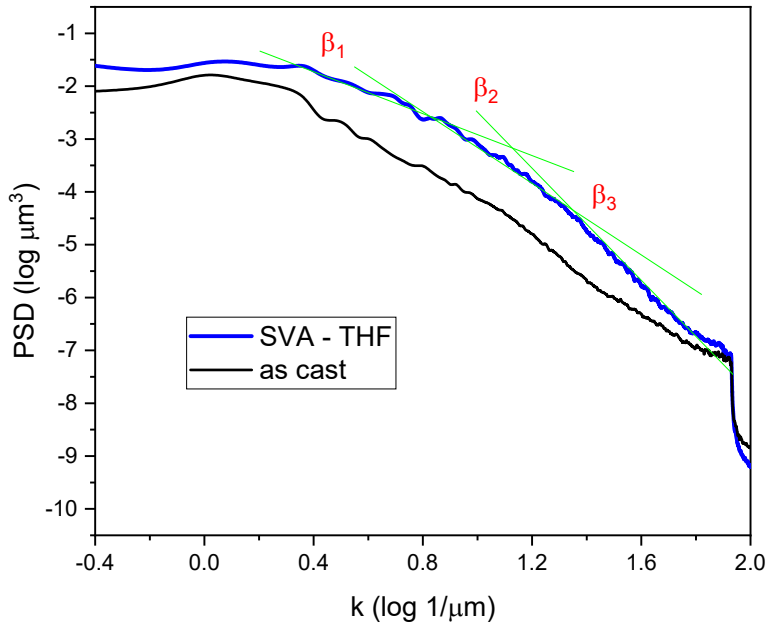

Figure S14 - PSD curves acquired from as cast or SVA-treated PBDTTT-CT:PDI-DPP-PDI films with THF. The green lines are theoretical fitting of linear functions.

Table S2 – Slopes from PDS curves and calculated D_s values

Film	Slope			D_s		
	β_1	β_2	β_3	D_{S1}	D_{S2}	D_{s3}
As cast	2.78	3.86		2.11	1.57	
SVA - THF	1.05	2.88	4.87	2.97	2.06	1.06

Table S3 – Photovoltaic parameter acquired from as cast and SVA-treated devices with THF.

Device	J_{sc} (mA/cm^2)	V_{oc} (V)	FF (%)	PCE (%)
As cast	6.50	0.79	27	1.35
SVA	9.40	0.89	37	3.10